Proc. Natl. Acad. Sci. USA
Vol. 90, pp. 7849–7853, August 1993
Biophysics

Two different forms of metarhodopsin II: Schiff base deprotonation precedes proton uptake and signaling state

(phototransduction/rhodopsin/retinal protein/receptor protein/G protein)

SOPHIA ARNIS AND KLAUS PETER HOFMANN†

Institut für Biophysik und Strahlenbiologie, Albert-Ludwigs-Universität, Albertstrasse 23, D-79104 Freiburg, Germany

Communicated by Walther Stoeckenius, April 28, 1993

ABSTRACT **Rhodopsin is a retinal protein and a G-protein-coupled receptor; it shares with both of these families the seven helix structure. To generate the G-interacting helix–loop conformation, generally identified with the 380-nm absorbing metarhodopsin II (MII) photoproduct, the retinal Schiff base bond to the apoprotein must be deprotonated. This occurs as a key event also in the related retinal proteins, sensory rhodopsins, and the proton pump bacteriorhodopsin. In MII, proton uptake from the aqueous phase must be involved as well, since its formation increases the pH of the aqueous medium and is accelerated under acidic conditions. In the native membrane, the pH effect matches MII formation kinetically, suggesting that intramolecular and aqueous protonation changes contribute in concert to the protein transformation. We show here, however, that proton uptake, as indicated by bromocresol purple, and Schiff base deprotonation (380-nm absorption change) show different kinetics when the protein is solubilized in suitable detergents. Our data are consistent with a two-step reaction:**

$$\mathrm{MI} \rightleftharpoons \mathrm{MII_a} \overset{+\,n\mathrm{H^+}}{\rightleftharpoons} \mathrm{MII_b}.$$

The first step, with an activation energy E_A = 160 kJ/mol, is linked to Schiff base deprotonation; it is endothermic and depends on the hydrophobic milieu around the protein. The second step is slightly exothermic; E_A = 60 kJ/mol and n = 2. The transformation of the protein determines the apparent pK_a of 6.75. From the known pH dependence of G-protein activation, we conclude that MII_a and MII_b must be successively formed to generate full catalytic activity for nucleotide exchange in the G protein.

The visual process in rods begins with the absorption of light in rhodopsin (Rh, A_{max} = 500 nm), an intrinsic membrane protein in the discs of the rod outer segment. Rh's chromophore retinal forms a protonated Schiff base with Lys-296, centrally located in the last of the seven transmembrane helices of the apoprotein (1). After rapid cis/trans isomerization of retinal, photoexcited Rh relaxes via intermediates with different chromophore–protein interaction and absorption spectra (2, 3). Metarhodopsin II (MII, A_{max} = 380 nm) forms in milliseconds; its Schiff base is still intact but deprotonated (2, 3). The deprotonation causes the absorption shift to 380 nm (4). It is mandatory for Rh to adopt a conformation in which it interacts with the G protein transducin (4, 5). The MII form remains active for minutes, in equilibrium with the 480-nm intermediate MI (3, 6). Kinetics (3, 6–9) and pH dependence (2, 6) of MII suggest the existence of isochromic MII species.

Besides the protonation change at the Schiff base, light induces the exchange of protons between Rh and the aqueous milieu (10). An initial uptake of protons occurs with kinetics similar to MII formation (11), and MII is favored above MI by acidic pH (2, 3). Schiff base deprotonation and proton uptake may contribute to one concerted reaction in the protein, which means that the spectroscopic species would not form without the accompanying "essential" protonation (2, 3, 6), according to the classical reaction scheme:

$$\mathrm{MI} + n\mathrm{H^+} \rightleftharpoons \mathrm{MII}, \qquad [1]$$

where $0.6 < n < 1.0$ (6), disregarding transient "nonessential" protonation changes (3, 6, 12). Differences in kinetics and pH dependence of MII formation and H^+ uptake, which contradict Eq. 1, were noted in earlier work (11, 13) but artefacts of the pH assay could not be excluded (11). In later studies on Rh and bacteriorhodopsin, artefacts have been shown to include delays due to H^+ diffusion to the indicator dye (14), the influence of local pH on the membrane surface (15), G-protein-dependent additional H^+ uptake (16), or the diffusional barrier of the disc membrane (17).

To avoid these problems, we have purified Rh in detergents with flexible alkyl chains. They accelerate the MII absorption change by two orders of magnitude, as compared to the native membrane environment or digitonin (18). If proton uptake is obligatory for the MII conformation change, it must be accelerated as well and maintain its kinetic match to MII formation. As will be shown below, this is not the case. Proton uptake occurs with significantly slower kinetics than MII formation, and its dependence on pH, temperature, and ionic strength identifies it as a requirement of a separate transformation of the protein.

MATERIALS AND METHODS

Sample Preparation. Disc membranes were isolated from bovine rod outer segments and Rh was solubilized and purified in octyl glucoside (OG) or dodecyl maltoside (DM), as described (18). The purified Rh was washed with buffer-free saline in an Amicon cell with YM-30 membrane.

Flash Photolysis. We used a two-wavelength flash photometer (16) and recorded the 380-nm and 595-nm absorption changes simultaneously in a two-channel digital oscilloscope (NIC 2090). All samples contained 2 μM Rh, 130 mM NaCl, and 12.3 μM bromocresol purple (BCP).

Calibration. Absorption changes were recorded at 380 nm for MII and at 595 nm for indicator dye BCP. To correct the proton uptake (ΔH^+) signals for photoproduct absorption at 595 nm (*ca.* 10%), we measured one unbuffered and one buffered aliquot for each sample, using 50 mM Hepes for pH 7 and 50 mM Mes for lower pH; the difference represents the pure ΔH^+ signal. The effect of the change of ionic strength by

The publication costs of this article were defrayed in part by page charge payment. This article must therefore be hereby marked "*advertisement*" in accordance with 18 U.S.C. §1734 solely to indicate this fact.

Abbreviations: OG, octyl glucoside; DM, dodecyl maltoside; Rh, rhodopsin; MII, metarhodopsin II; MII signal, absorption change due to MII formation; ΔH^+ signal, indicator absorption change due to proton uptake by Rh; BCP, bromocresol purple.

†To whom reprint requests should be addressed.

the buffer is negligible and the ΔH^+ does not contribute significantly to the MII signal of the unbuffered sample, because the BCP absorption changes negligibly at 380 nm and the indicator dye does not affect the absorption change in the protein.

The ΔH^+ signal was calibrated by adding small amounts of HCl (4.3 μM) to the dark sample, as described (16).

EXPERIMENTAL RESULTS

Separation of ΔH^+ and MII in Detergents. We have simultaneously measured the flash-induced absorption change at 380 nm (MII signal) due to deprotonation of the Schiff base and the absorption change at 595 nm (ΔH^+ signal) indicating the pH change in the medium due to proton uptake. In washed disc membranes, the signals have similar kinetics (data not shown); only at high temperatures ΔH^+ is slightly slower than MII.

However, for purified Rh, solubilized in OG, the half mean time of MII formation is τ(MII) = 1 ms; the one of proton uptake is $\tau(\Delta H^+)$ = 25 ms. In DM, we find τ(MII) = 7 ms and $\tau(\Delta H^+)$ = 25 ms (Fig. 1). In both detergents, computer fits for the MII signals yielded approximately biphasic kinetics with a dominating fast component.

The important qualitative conclusion from Fig. 1 is that a species with 380-nm absorption—i.e., with a deprotonated retinal Schiff base bond—can be almost completely formed while proton uptake, as indicated by the ΔH^+ signal, is still far from its completion.

Kinetic Analysis of MII and ΔH^+. *ΔH^+ signals are slower than H^+ diffusion.* The observed kinetics of proton uptake is so slow that it cannot be explained by diffusion time. For bacteriorhodopsin, the transfer times of aqueous H^+ to the indicator dye pyranine were maximally 1 ms (14). The fact that the ΔH^+ signals are much slower provides a first indication for a separate transition in the protein, linked to proton uptake.

Arrhenius plots. This notion is further corroborated by measurements of MII formation and pH effect in DM at temperatures between −10°C and 40°C. Arrhenius plots for the MII signal show a straight line (Fig. 2). For ΔH^+, it can be approximated by two linear sections, with activation energies E_{Aa} and E_{Ab}. At temperatures below *ca.* 8°C, the plot for ΔH^+ approximates the one for MII, indicating that MII formation becomes the rate-limiting step.

From MII signals in DM, we obtain an activation energy of E_{Aa} = 156 kJ/mol, similar to native membranes (6, 9), in spite of the quite different reaction rate. The same E_{Aa} was found in OG within the measurable temperature range (data not shown). The slope of ΔH^+ above *ca.* 8°C indicates a reaction with E_{Ab} = 63 kJ/mol. The relatively large E_{Ab} provides strong further evidence for a separate transformation in the protein, reflected in the H^+ uptake.

Sigmoidal time course. In DM, ΔH^+ signals, measured at low temperatures and at sufficiently high pH (pH > 6.8), assume a sigmoidal time course (Fig. 2 *Inset*). It can be approximated by a two-step reaction A → B → C. Computer

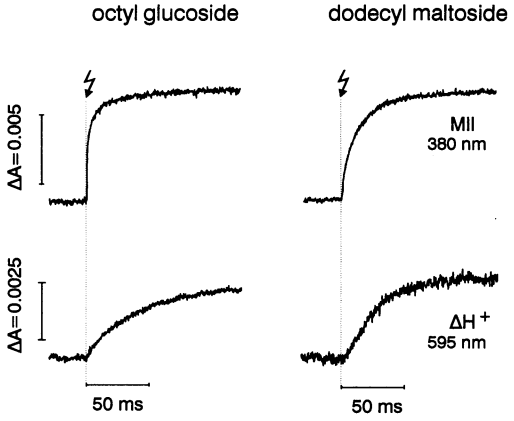

FIG. 1. Kinetics of MII formation and proton uptake (ΔH^+) in solutions of purified Rh, solubilized in OG or DM. Both reactions were simultaneously measured at pH 7, 3°C; OG and DM were 50 mM and 0.4 mM, respectively.

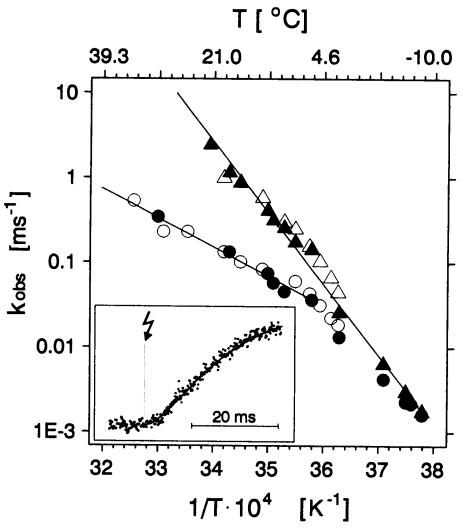

FIG. 2. Kinetics of MII and ΔH^+ in purified Rh in DM. (*Inset*) Measured example on an expanded time scale, recorded at T = 5°C, pH 7, in 0.4 mM DM. A computer fit to the data, according to an A → B → C scheme (see text), is overlaid with the data. In the Arrhenius plot, triangles and circles represent the observed rate k_{obs} (inverse reaction time, $\ln 2/\tau_{1/2}$) of MII and ΔH^+, respectively. Freezing was prevented by sucrose; closed symbols, samples with 25% sucrose; open symbols, without sucrose.

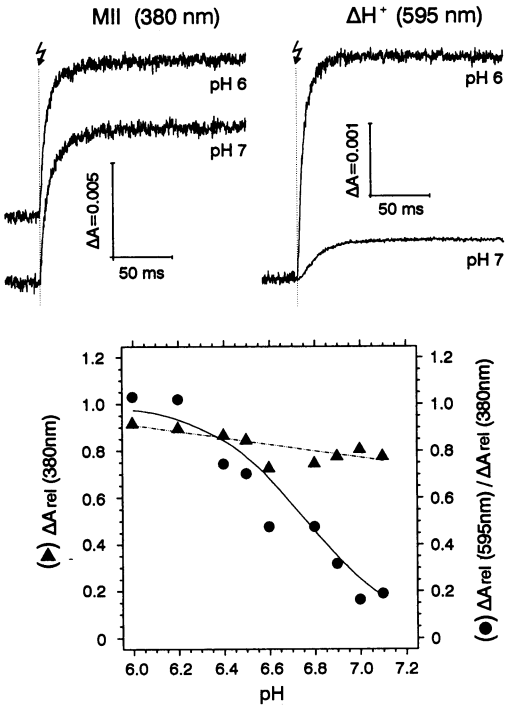

FIG. 3. pH dependence of MII and ΔH^+ in purified Rh in DM. (*Upper*) Typical signals. (*Lower*) MII signals are plotted on relative scales ($\Delta A_{rel} = \Delta A/\Delta A_{max}$, where ΔA_{max} is the maximally possible amplitude of the respective signal). T = 5.5°C; 0.4 mM DM. The solid line fits Eq. 3c; the dotted line is a linear regression.

calculations with MII and ΔH^+ signals for steps A → B and B → C, respectively, gave good fits. The irreversible two-step scheme is a first approximation to the equilibration scheme given below (Eq. 2).

pH and Temperature Dependence. Fig. 3 shows MII and ΔH^+ signals recorded at pH 6 and 7. Under the conditions, only the ΔH^+ signal depends markedly on pH. Lowering the pH by one unit accelerates this signal about 10-fold, with a corresponding increase of the final amplitude. The curves in Fig. 3 *Lower* show the titration of proton uptake and MII formation. The lines are computer fits to the data, using a linear regression for MII and a hyperbolic function for ΔH^+, which plots an equilibrium between a protonated and unprotonated species, separated from one another by a free energy gap (see below, Eqs. 3). The resulting titration curve yields an apparent pK of 6.75. The maximal H^+ uptake is 2 H^+ per photolyzed Rh, consistent with the quadratic fit to the titration curve in Fig. 3.

For the temperature dependence we find MII amplitudes virtually independent of temperature, while the relative amplitude of ΔH^+ decreases from 0.65 (−10°C) to 0.35 (50°C) (pH 6.5; Fig. 4). Model fits (Eq. 4) from data at pH 6, 6.5, and 7.0 yield the reaction enthalpy.

Ionic Strength Dependence. The MII and the ΔH^+ signal depend on ionic strength. We have found that the MII signal accelerates with increasing ionic strength, with almost constant amplitude, whereas ΔH^+ decreases with an IC_{50} = 500 mM (NaCl) (Fig. 5).

Reaction Scheme. The experimental results are consistent with a reaction scheme where proton uptake and release can only occur via the product MII_a:

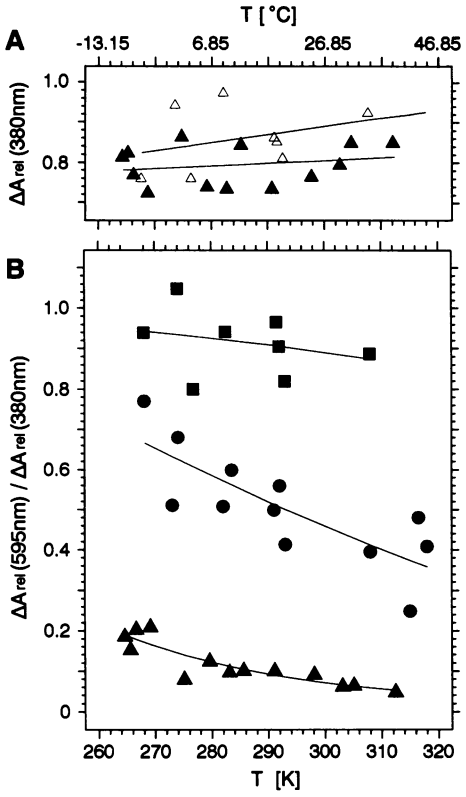

FIG. 4. Temperature dependence of MII formation and ΔH^+ in solutions of purified Rh, in DM. (*A*) Amplitudes of MII signals, plotted on relative scales ($\Delta A_{rel} = \Delta A/\Delta A_{max}$, where ΔA_{max} is the maximally possible amplitude of the respective signal), at pH 7 (closed triangles) and pH 6 (open triangles). (*B*) Amplitudes of ΔH^+ signals, normalized as in *A*. The different symbols belong to pH 7 (triangles), pH 6.5 (circles), and pH 6.0 (rectangles). Data points in *A* and *B* are from simultaneous measurements. The solid lines plot Eqs. 3c and 4.

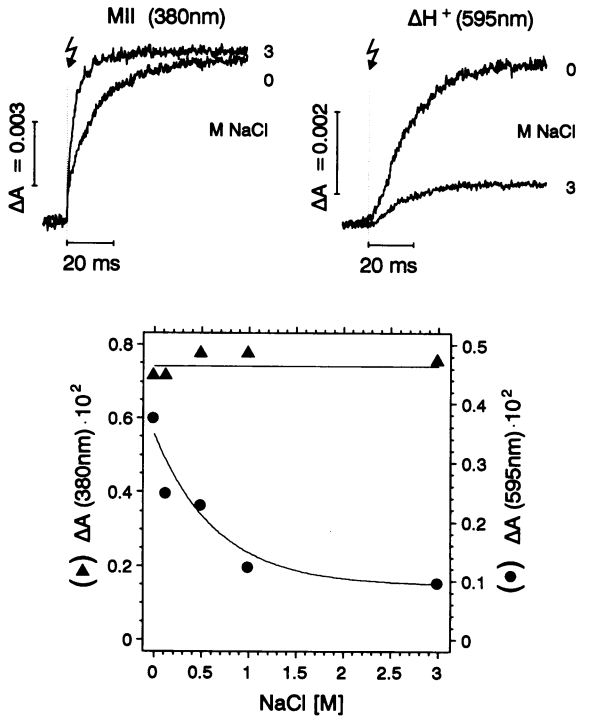

FIG. 5. Ionic strength dependence of MII and ΔH^+ in DM-solubilized Rh. (*Upper*) Examples of recorded signals, at scales that allow kinetic comparison. (*Lower*) MII and ΔH^+ signals are plotted on a ΔA scale. Both reactions were simultaneously measured at 4°C, pH 7.

$$MI \underset{k_{a2}}{\overset{k_{a1}}{\rightleftharpoons}} MII_a \underset{k_{b2}}{\overset{k_{b1}\ +\ nH^+}{\rightleftharpoons}} MII_b. \qquad [2]$$

The spectrophotometrically observed MII is the sum of MII_a and MII_b.

With $k_{b1} = k'_{b1}\,[H^+]^n$ (pseudo-first order), we can define equilibrium constants: $K_a = [MII_a]/[MI]$; $K_b = MII_b/([MII_a]\cdot[H^+]^n) = K'_b\cdot(1/[H^+]^n)$.

This yields ΔG° for steps a and b:

$$\ln K_a = -\Delta G^\circ_a/RT \qquad [3a]$$

$$\ln K_b = -\Delta G^\circ_b/RT - 2.3\cdot n\cdot \mathrm{pH}. \qquad [3b]$$

To fit the data in Fig. 3, we used the equation (ref. 6; for ΔA_{rel} see *Appendix*):

$$\Delta A_{rel}(595)/\Delta A_{rel}(380) = 1/[1 + \exp(\Delta G^\circ_b/RT + 2.3\cdot n\cdot \mathrm{pH})]. \qquad [3c]$$

This fit yields ΔG° and n (and, hence, $\Delta G^\circ_{pH} = RT\cdot 2.3\cdot n\cdot$pH) for the reaction $MII_a \rightleftharpoons MII_b$ in Table 1. At pH 6.75, ΔG°_{pH} and ΔG° balance each other, so that $K = 1$; this is the apparent pK of the protonatable groups. Note that the SEM of the ΔG (±5 kJ/mol) means an uncertainty of the apparent pK in the titration curve of ±0.4 pH unit (Fig. 3).

To obtain ΔH° for $MII_a \rightleftharpoons MII_b$ in Table 1 from fits of the temperature dependence (Fig. 4), one uses Eq. 3c and

$$\Delta G^\circ/RT = \Delta H^\circ/RT + \Delta S^\circ/R. \qquad [4]$$

ΔH° and ΔG° for $MI \rightleftharpoons MII_a$ carry large errors, mainly from K_a (*Appendix*).

One obtains the free activation energy $\Delta G^\#$ (Table 1) by analogy to Eq. 3b from the equilibrium constant of absolute

Table 1. Thermodynamic parameters of transitions between metarhodopsin forms

Reaction	Thermodynamic parameter		
	ΔH°	ΔG°_{pH}	ΔG°, kJ/mol
MI ⇌ MII_a*	55 ± 17	0	1 ± 23
MII_a ⇌ MII_b†	−20 ± 3	64/72/80 ± 5‡	−72 ± 5
	$\Delta H^\#$	$\Delta G^\#_{pH}$	$\Delta G^\#$, kJ/mol
MI ⇌ MII_a§	156 ± 4	0	67/57/53 ± 2
MII_a ⇌ MII_b†	61 ± 3	32/36/40 ± 2‡	32/28/24 ± 2‡

All values are for T = 5°C; R = 8.3 J·mol^{-1}·K^{-1}. The parameters were determined in samples as indicated. $\Delta G^\#$, free activation energy.
*Washed membranes (for the large error of ΔH° and ΔG°, see text).
†DM.
‡At pH 6.0, 6.75, and 7.5, respectively.
§Washed membranes, DM and OG.

rate theory (see ref. 6 and citations therein). Since the on rate of the ΔH^+ signal is 10 times faster at pH 6 than at pH 7, $n^\#$ = 1; $\Delta H^\# = E_A - RT$.

Limits of the Description. (*i*) The data exclude the net uptake of protons in forming MII_a but not a catalytic protonation during the transition (13), leading to a complex pH dependence of the overall reaction (6). (*ii*) Eq. 2 describes only the rapidly formed MII species, but not the slow MII intermediate (3) arising in seconds (from MII_b). (*iii*) Even on the time scale of milliseconds, a more complex scheme may apply (19). Note, however, that the observed slow MII signal component, similar to the ΔH^+ signal kinetics, is expected from Eq. 2, when MII_b molecules reenter the spectrally visible transition MI → MII_a via the back reaction MII_b → MII_a.

DISCUSSION

Proton Uptake from the Aqueous Phase Is Not Required to Form MII. The light-induced proton uptake by rhodopsin occurs after the 380-nm photoproduct is already formed. Essential protons from the aqueous phase are not required for its formation, as previously assumed (2, 3, 6). Since the 380-nm absorption change reflects the deprotonation of the retinal Schiff base bond to the apoprotein during the MI/MII conversion (4), we conclude that the proton uptake from the medium occurs after the internal proton translocation. Models requiring one concerted reaction in the protein, which involves both proton movements, do not apply.

Proton Uptake Occurs in a Separate, Later Transformation. The barrier to the internal translocation of the Schiff base proton dominates the overall MI/MII conversion in membranes. When this barrier is lowered in detergent, a separate transformation of the protein emerges by the biphasic Arrhenius plot and the sigmoidal kinetics of proton uptake. The classical scheme in Eq. 1 must be replaced with the two-step scheme in Eq. 2 (illustrated in Fig. 6).

The Two Reaction Steps Depend Differently on the Molecular Environment. In Fig. 6, formation of state MII_a requires translocation of the Schiff base proton to another internal group within Rh's hydrophobic core. Only in MII_b does the protein assume a conformation that requires and/or results in the additional net uptake of aqueous protons.

The transition to MII_a bears the dependence of the MI/MII conversion on the membraneous or micellar host. It has been related to a free volume change in the hydrophobic space (18, 20), as symbolized in Fig. 6 by the lateral expansion. Its large activation energy and standard free energy change (Table 1) indicate a major conformational change. The parallel shift of the Arrhenius plot in different detergents shows that its thermal activation is mainly entropy driven. It is also the step responsible for the known endothermic characteristics (2, 3) of the MI/MII conversion.

The transition to MII_b may determine the dependence of MII on properties of the aqueous phase, as was shown for pH and ionic strength. The data fit the simplest idealized scheme, in which (*i*) MII_a is always unprotonated and MII_b is always protonated (2 H^+) and (*ii*) the free energy gap is the sum of a pH-dependent and a pH-independent term (ΔG°_{pH} and ΔG° in Eqs. 3 and Table 1). The dependence on ionic strength indicates the exposure of negative charges in MII_b, consistent with the measured protonation change.

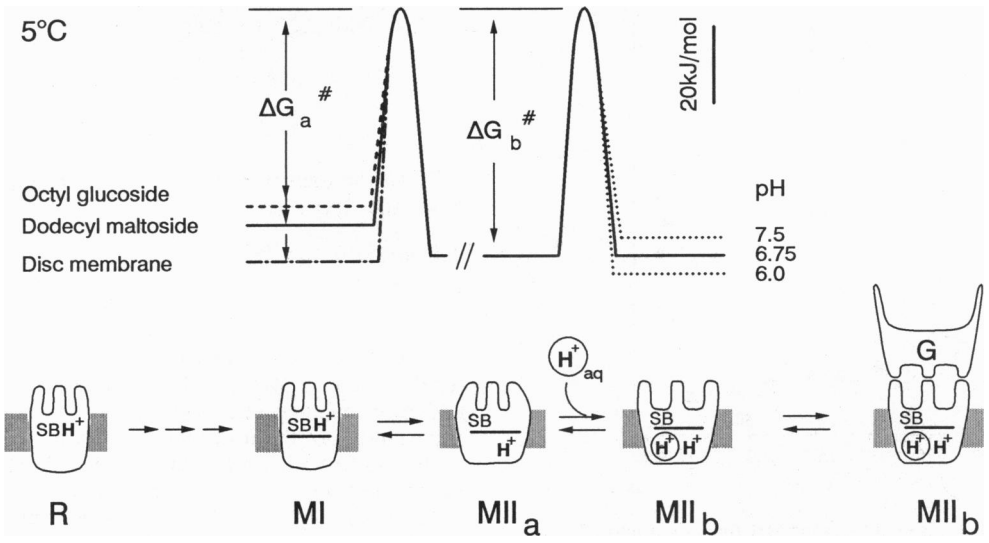

FIG. 6. Free energy scheme and reaction model of metarhodopsin conformations. (*Upper*) Free energy levels and barriers for the MII intermediates MI, MII_a, and MII_b. They were taken from the free energy gaps (sum of $\Delta G^\circ_{pH} = RT \cdot 2.3 \cdot n \cdot pH$ and the intrinsic ΔG°) and the activation free energies in Table 1. The MII_a level relative to MI cannot be determined with accuracy (Table 1) and is omitted. (*Lower*) Reaction model illustrating how the G protein activating form of Rh develops. After Rh and fast intermediates (not shown), the metarhodopsin products are successively formed: MI, sterically triggered, as symbolized by the horizontal bar; retinal Schiff base, SB (still protonated); MII_a (SB deprotonated and change of free volume in the hydrophobic core of the membrane); and MII_b (like MII_a, but with an additional conformational change presenting the G-compatible helix–loop structure). Only one of the two aqueous H^+ bound to MII_b is shown; its location is unknown.

Catalytic Activity Requires Both Reaction Steps. The functional importance of the second reaction step follows from its pH dependence. Rh's activity as a catalyst of nucleotide exchange in the G protein mimics the actual pH-dependent amount of MII in its equilibria with MI and MIII (3, 6), in the native membrane (21), and in DM micelles (ref. 22; S. Jäger, S.A., and K.P.H., unpublished data). The titration curves for the G-protein activation rate and for the formation of MII_b from its precursor MII_a (Fig. 3) resemble each other. The low pH required to form MII_b (Fig. 3) may surprise; however, the surface pH on disc membranes will be lower than the cytoplasmic bulk pH (15).

We propose (see Fig. 6) that the $MII_a \rightarrow MII_b$ transition reflects the development of the helix–loop conformation that produces the three-loop interaction pattern of MII–G interaction (1). This independent second transition can explain why mutants can exist that are impaired in the interaction with transducin but show an apparently normal 380-nm absorption change (1, 23).

Resulting Questions. Interesting properties of the MII state remain to be assigned to MII_a or MII_b. They include (*i*) the altered orientation of the chromophore, (*ii*) electrical effects occurring at the time scale of MII formation, (*iii*) the access of small solutes to the chromophore, (*iv*) the net volume change of the protein, and (*v*) FTIR bands related to other than chromophoric groups (3, 24).

Finally, when we compare Rh to the bacterial rhodopsins, the H^+ uptake may be viewed as incomplete proton pumping. Translocation of the Schiff base proton is a necessary precursor of the aqueous proton movement, like in bacteriorhodopsin, where kinetic evidence exists for two distinct M states (25). Bacterial sensory rhodopsins share with Rh a steric trigger mechanism, which mediates between retinal isomerization and the signaling conformation (24, 26). Moreover, the transducer protein associated with bacterial sensory rhodopsin I influences the protonation of the Schiff base (27), analogous to G-protein-dependent extra MII in Rh (3, 23). The two-step mechanism described here may apply more generally.

APPENDIX

Eq. **3c** is based on relations between the relative amplitudes of the absorption signals (Fig. 3) and the equilibrium constants K_a and K_b. From

$$\Delta A_{rel}(380) = ([MII_a] + [MII_b])/([MI] + [MII_a] + [MII_b])$$

$$\Delta A_{rel}(595) = [MII_b]/([MI] + [MII_a] + [MII_b]),$$ one obtains

$$K_a = \{\Delta A_{rel}(380) - \Delta A_{rel}(595)/[1 - \Delta A_{rel}(380)]\}$$

$$K_b = \Delta A_{rel}(595)/[\Delta A_{rel}(380) - \Delta A_{rel}(595)].$$

See ref. 6 for k_{a1}, k_{b1}, and k_{obs}.

We thank Herbert Gutfreund and Oliver Ernst for discussions and Inge Bäumle for technical assistance. This work was supported by a grant from the Deutsche Forschungsgemeinschaft (SFB 60, H-5, to K.P.H.).

1. Hargrave, P. A., Hamm, H. E. & Hofmann, K. P. (1993) *BioEssays* **15**, 43–50.
2. Matthews, R. G., Hubbard, R., Brown, P. K. & Wald, G. (1963) *J. Gen. Physiol.* **47**, 215–240.
3. Hofmann, K. P. (1986) *Photobiochem. Photobiophys.* **13**, 309–338.
4. Doukas, A. G., Aton, B., Callender, R. H. & Ebrey, T. G. (1978) *Biochemistry* **17**, 2430–2435.
5. Longstaff, C., Calhoon, D. & Rando, R. R. (1986) *Proc. Natl. Acad. Sci. USA* **83**, 4209–4213.
6. Parkes, J. H. & Liebman, P. A. (1984) *Biochemistry* **23**, 5054–5061.
7. Straume, M., Mitchell, D. C., Miller, J. L. & Litman, B. J. (1990) *Biochemistry* **29**, 9135–9142.
8. Lewis, J. L. & Kliger, D. S. (1992) *J. Bioenerg. Biomembr.* **24**, 201–210.
9. Hoffmann, W., Siebert, F., Hofmann, K. P. & Kreutz, W. (1978) *Biochim. Biophys. Acta* **503**, 450–461.
10. Radding, C. M. & Wald, G. (1965) *J. Gen. Physiol.* **39**, 909–933.
11. Wong, J. K. & Ostroy, S. E. (1973) *Arch. Biochem. Biophys.* **154**, 1–7.
12. Bennett, N. (1980) *Eur. J. Biochem.* **111**, 99–103.
13. Emrich, H. E. & Reich, R. (1974) *Z. Naturforsch. Teil C* **29**, 577–591.
14. Heberle, J. & Dencher, N. A. (1992) *Proc. Natl. Acad. Sci. USA* **89**, 5996–6000.
15. Szundi, I. & Stoeckenius, W. (1989) *Biophys. J.* **56**, 369–383.
16. Schleicher, A. & Hofmann, K. P. (1985) *Z. Naturforsch. Teil C* **40**, 400–405.
17. Kaupp, U. B., Schnetkamp, P. P. M. & Junge, W. (1981) *Biochemistry* **20**, 5511–5516.
18. König, B., Welte, W. & Hofmann, K. P. (1989) *FEBS Lett.* **257**, 163–166.
19. Thorgeirsson, T. E., Lewis, J. W., Wallace-Williams, S. E. & Kliger, D. S. (1992) *Photochem. Photobiol.* **56**, 1135–1144.
20. Mitchell, D. C., Straume, M., Miller, J. L. & Litman, B. J. (1990) *Biochemistry* **29**, 9143–9149.
21. Parkes, J. H. & Liebman, P. A. (1982) *Invest. Ophthalmol. Visual Sci.* **22**, Suppl. 44 (abstr.).
22. Fahmy, K. & Sakmar, T. P. (1993) *Biochemistry* **32**, 7229–7236.
23. Franke, R. R., König, B., Sakmar, T. P., Khorana, H. G. & Hofmann, K. P. (1990) *Science* **250**, 123–125.
24. Siebert, F. (1992) in *Biomolecular Spectroscopy: Advances in Spectroscopy*, eds. Clark, R. J. H. & Hester, R. E. (Wiley, Chichester, England).
25. Lanyi, J. K. (1992) *J. Bioenerg. Biomembr.* **24**, 169–179.
26. Yan, B., Nakanishi, K. & Spudich, J. L. (1991) *Proc. Natl. Acad. Sci. USA* **88**, 9412–9416.
27. Yao, V. J. & Spudich, J. L. (1992) *Proc. Natl. Acad. Sci. USA* **89**, 11915–11919.